flow were monitored by the use of a laser speckle blood flow imaging system (Omegazone, Omegawave), **as previously reported, but with some modifications.**[6, 7] In the day prior to the first day of CBF measurement anesthesia was induced with 4% halothane and maintained with 1.5% halothane in 80% nitrous oxide and 20% oxygen, the skull was exposed by a midline scalp incision **and the scalp reflected laterally;** the scalp **was** kept open throughout the experiment. During the measurement of CBF, the **intact** skull surface was diffusely illuminated by 780 nm laser light. The scattered light was filtered and detected by a CCD camera positioned over the head. The filter detected only scattered light that had a perpendicular polarization to the incident laser light. The raw speckle images were used to compute speckle contrast, which corresponds to the number and velocity of moving red blood cells, approximating CBF. Signal processing was performed by the algorithm developed by Forrester et al.[8] Color-coded blood flow images were obtained in high-resolution mode (639 × 480 pixels; 1 image/sec). The sample frequency was 60 Hz. One blood flow image was generated by averaging numbers obtained from 20 consecutive raw speckle images. The recordings were initiated after the examiner confirmed that CBF did not change over 1 minute, and the five recordings of blood flow image were averaged. In order to prevent the fluctuation of CBF and blood pressure during the measurement of CBF, anesthesia was induced with 1.5% halothane and maintained with the same concentration of halothane in 80% nitrous oxide and 20% oxygen. During the measurement of CBF, blood pressure was measured by the tail cuff method and confirmed to be kept constant. Rectal temperature was maintained between 36.5°C and 37.5°C. In addition, the stability of the level of anesthesia was checked by testing corneal reflexes and motor responses to tail pinch.

Visualization of cerebral angioarchitecture

The cerebral angioarchitecture was studied by a modification of the postmortem latex perfusion technique on day 7 after the surgery.[9-14] The root of the ascending aorta was cannulated with flexible

plastic tubing (0.65 mm external diameter). The tubing was connected to a 5 mL syringe, the cannulated aorta, and a mercury manometer, establishing a closed circuit to monitor perfusion pressure. A lethal dose of papaverine hydrochloride (40 to 50 mg/kg) was injected to produce maximal vasodilation. Immediately after 2 mL saline injection, 4 mL white latex compound (Chicago Latex Products) mixed with 50 μL/mL carbon black (Fueki) diluted 2:1 with saline was injected at a perfusion pressure of 150 mm Hg over a 5-minute period. After the initiation of infusion, the right atrium of the heart was incised to allow for venous outflow. The injected volume of latex, as well as the time taken to harden the latex sufficiently, was much greater than those of previous reports (0.4–2 mL, 2 minutes).[9, 10, 13] In order to harden the latex completely for the brain removal procedure, the dead animal was soaked in ice-cold water 20 minutes after the end of infusion, and the brain was subsequently removed 20 minutes later. Photographs of the dorsal and ventral surface of the brain were taken using a digital microscope (DinoLite, AnMo Electronics Corp.) at ×80 magnification. The vessel diameters of the leptomeningeal anastomoses and the circle of Willis were measured using image analysis software (DinoCapture, AnMo Electronics Corp.). The distal MCA was identified from its branch angle and distinguished from the distal ACA or posterior cerebral artery (PCA). The maximal diameter of the leptomeningeal anastomoses was measured at the point of confluence between the distal MCA and the distal ACA (Heubner's anastomoses) or between the distal MCA and the distal PCA. The point of confluence was defined as the narrowest part of the vessel or half way between the nearest branching points of the ACA, the MCA, and the PCA branches, respectively. The diameter of the internal carotid artery (ICA), ACA, MCA and the posterior communicating artery (Pcom) were averaged across both sides. The diameters of the ICA and MCA were measured just proximally and distally to the terminal bifurcation of the ICA, respectively. The diameter of the ACA was measured just proximally to the origin of the olfactory artery. The diameter of the Pcom was measured at its origin from the ICA.

Histologic and immunohistochemical evaluation

Mice were euthanized 7 and 28 days after the surgery. The harvested brains were subjected to histologic examination using a standard procedure described elsewhere.[2] Klüver–Barrera (KB) staining was used to observe any histological changes. The severity of the white matter (WM) lesions was semiquantitatively graded into four levels by an investigator blind to the experimental condition.[2]

Primary antibodies used for immunohistochemistry included those against: the astrocyte marker, glial fibrillary acidic protein (GFAP) (1:10000, Dako Cytomation); the microglia marker, ionized calcium binding adapter molecule 1 (Iba-1) (1:500, Wako Pure Chemical Inductries); the mature oligodendrocyte marker, glutathione-S-transferase-pi (GST-pi) (1:10000, Stressgen); the oxidative DNA damage marker, 8-hydroxy-deoxyguanosine (8-OHdG) (1:100, Japan Institute For the Control of Aging); and the endothelial marker, platelet endothelial cell adhesion molecule (PECAM)-1 (CD31) (1:100, Pharmingen). In the sections immunostained for GFAP, Iba-1, and GST-pi, we counted the number of immunopositive cells in six fields (cells/0.25 mm^2) in the median and the paramedian part of the corpus callosum and the anterior commissure at 0 to 0.5 mm anterior from the bregma. Capillary density was quantified by the number of PECAM-1-positive cells (cells/mm^2). Vessels with a diameter between 3 and 8 μm were counted. The vessel counts were performed in ten fields in the cerebral cortex, the corpus callosum, and the caudoputamen of the coronally-cut sections at 0 to 0.5 mm anterior from the bregma.

Analysis of oxidative damage in cerebral vessels

To evaluate oxidative damage in cerebral microvessels, double immunofluorescence staining for PECAM-1 and 8-OHdG was performed on day 3 post-BCAS. The acquired images were processed using Adobe Photoshop (version 7, Adobe System). RGB images were converted to 8-bit grayscale images. Based on an analysis of pixel fluorescence intensities, which ranged from 0 to 255, specific staining was distinguished from background by using a threshold value of 45–50 for 8-OHdG and

30–35 for PECAM-1. Area densities of structures stained with 8-OHdG or PECAM-1 were calculated as the proportion of pixels having a fluorescence intensity value equal to or greater than the threshold. Four fields in the corpus callosum of the coronally-cut sections at 0 to 0.5 mm anterior from the bregma were examined and the number of pixels with 8-OHdG positivity per the number of pixels with PECAM-1 positivity was calculated.

Analysis of monocyte recruitments and proliferation of smooth muscle cells

On day 7 post-BCAS, mice were euthanized by intracardiac perfusion with 4% paraformaldehyde in 0.1 mol/L phosphate buffer (PB, pH 7.4). The brains were post-fixed in 4% paraformaldehyde in 0.1 mol/L PB, and were stored in 20% sucrose in 0.1 mol/L PB (pH 7.4). The brains were embedded in paraffin and sliced into 6 μm-thick coronal sections and then subjected to the immunofluorescent analysis for Ki-67 and F4/80 together with α-smooth muscle actin (α-SMA). Afterdeparaffinization with xylene and rehydration with ethanol,[15] antigen retrieval for the Ki-67 antigen was performed using 0.01 mol/L citrate buffer (pH 6.0) at 95°C for 20 minutes. Sections were rinsed briefly with 0.1 mol/L PBS, pH 7.4, and then blocked for 30 minutes at room temperature in a solution of PBS containing 5% preimmune serum and 0.3% Triton-X100 (PBS+). Sections were subsequently incubated at 4°C for 24 hours with primary antibodies diluted in PBS+ then washed thoroughly with PBS at room temperature. Sections were incubated with secondary fluorochrome-conjugated antibodies in PBS for 90 minutes at room temperature then washed thoroughly. Stained tissue sections were evaluated by using a confocal laser-scanning device (FV1000, Olympus). The density of the Ki-67-immunoreactive smooth muscle cells (SMCs) per total SMCs was analyzed on the dorsal surface of the brain in the coronally-cut sections at 0.5 to 1 mm posterior from the bregma. In addition, the density of SMCs surrounded by F4/80-immunoreactive monocyte/macrophages was calculated per total SMCs on the same area of another section. Primary antibodies used for immunofluorescent

analysis were as follows: goat antibody to Ki-67 (1:100, Santa Cruz); rat antibody to F4/80 (10 μg/mL, Abcam); mouse antibody to α-SMA (1:100, Neomarkers). Secondary antibodies used were as follows: FITC-conjugated chicken antibody to goat IgG (1:100, Santa Cruz); FITC-conjugated chicken antibody to rat IgG (1:100, Santa Cruz); TRITC-conjugated rabbit antibody to mouse IgG (1:100, Dako Cytomation).

Y maze test

The Y maze test was performed at 1 month after the surgery in a manner similar to that described previously.[16] The Y maze is a three-arm maze with equal angles between all arms that is used to evaluate working memory. Mice were initially placed within one arm and allowed to move in the maze freely. The sequence and number of arm entries were recorded for each mouse over an 8-minute period. The percentage of triads in which all three arms were represented (ABC, CAB, or BCA but not BAB) was recorded as an alternation to estimate short-term memory of the last arms entered. The total number of possible alternations is the number of arm entries minus two. Furthermore, the number of arm entries serves as an indicator of spontaneous activity.

Eight-arm radial maze test

The 8-arm radial maze test was started at 1 month after BCAS. The test was conducted in a manner similar to that described previously.[17] Each arm (8×35 cm) radiated from an octagonal central starting platform (perimeter 10×8 cm). Identical food wells were used (1 cm deep and 2.1 cm in diameter). One week before pretraining, animals were deprived of food until their body weight was reduced to 75–85% of the initial level. Pretraining started on the eighth day. Each mouse was placed in the central starting platform and allowed to explore and to consume food pellets scattered on the whole maze for a 5-minute period (one session per mouse). After completion of the initial pretraining, mice received another pretraining to take a pellet from each food well after being placed at the distal end of each arm.

A trial was finished after the subject consumed the pellet. This was repeated eight times, using eight different arms, for each mouse. After these pretraining trials, actual maze acquisition trials were performed. All eight arms were baited with food pellets. Mice were placed on the central platform and allowed to obtain all eight pellets within 25 minutes. A trial was terminated immediately after all eight pellets were consumed or 25 minutes had elapsed. An "arm visit" was defined as traveling for >5 cm from the central platform.

cAMP assay

cAMP levels in the forebrain were determined by the radioimmunoassay method as previously described.[18] Mice were euthanized 5 days after surgery, the brain removed and frozen with liquid nitrogen, then preserved at –80°C. About 100 mg of frozen forebrain tissue was homogenized and extracted twice with 1 mL of ice-cold 0.1 N HCl solution. After centrifugation at 3000 rpm for 15 minutes at 4°C, the amounts of cAMP in the mixed supernatant was determined by radioimmunoassay using Yamasa cAMP assay kits (Yamasa).

Analysis of VEGF and bFGF protein expression in the forebrain

Western blot analysis of vascular endothelial growth factor (VEGF) and basic fibroblast growth factor (bFGF) was performed using protein extracts from the forebrain tissue of sham- and BCAS-operated mice on days 1 and 5. Forebrain tissue was homogenized in RIPA buffer (1X PBS, 1% Igepal, 0.5% sodium deoxycholate and 0.1% SDS with protease and phosphatase inhibitors (Sigma)) Homogenates were centrifuged at 10,000 x g for 15 minutes at 4°C to remove insoluble proteins and fibrous tissue, and protein content for each sample was determined using bicinchoninic acid (BCA protein assay; Pierce-Rockford). Samples were separated by SDS-PAGE on 10% gels then transferred to PVDF membranes. Membranes were blocked in 5% non-fat dry milk for 30 minutes at room temperature then incubated with anti-VEGF antibody (0.5 μg/mL, R&D systems) or anti-bFGF antibody (1:200,

Santa Cruz), and with **anti-β-tubulin antibody (1:1000, Sigma)**, which served as an internal control, at 4°C overnight. Immunoblots were then incubated with horseradish peroxidase-conjugated secondary antibody (1:10,000, Santa Cruz) for 1 hour at room temperature. Immunoblots were detected using Enhanced Chemiluminescence (ECL) Western Blotting Detection reagent (Amersham). ECL blots were digitally captured with a LAS-3000 imaging system (Fujifilm). The LAS-3000 imaging system has a CCD camera which is equipped with shading correction without automatic gain control, and has an ample and linear dynamic range (from 0 to 4.0 OD values). Images were processed using Multi Gauge v3.1 software (Fujifilm). The intensity of each band was determined by measuring the AUC-BG/mm^2 (AUC: area under the curve, BG: background). Anti-VEGF antibody detected only one band at about 30 kDa, anti-FGF antibody detected only one band at about 18 kDa, **and anti-β-tubulin antibody detected only one band at about 50 kDa**.

Quantitative real-time RT-PCR analysis of the forebrain

Total RNA was extracted from the forebrain tissue obtained from sham and BCAS-operated mice on days 1 and 5 using QIAzol Reagent (QIAGEN), following standard protocol.[19] Quantitative real-time RT-PCR analysis was carried out using an ABI PRISM 7300 Sequence Detection System (Applied Biosystems) with SYBR Green (Toyobo) or TaqMan probe, and values were normalized to 18S rRNA (TaqMan Ribosomal RNA Control Reagents VIC Probe; Applied Biosystems) to evaluate the levels of **AM,** calcitonin receptor-like receptor (CRLR), receptor activity-modifying protein (RAMP) 2, RAMP3, VEGF, and bFGF. The primers and probes used for quantitative real-time RT-PCR Analysis were as follows: **mouse AM forward, 5'-TACACGGGGACCTACAATGCT-3'; mouse AM reverse, 5'-TCGCACAGCTTGGTACGCTT-3'; mouse AM probe, 5';** mouse CRLR forward, 5'-GCTGGAATGACGTTGCAGC-3'; mouse CRLR reverse, 5' –GCCTTCACAGAGCATCCA-3'; RAMP2 forward, 5'-CCGGAGTCCCAGAATCAATCT-3'; mouse RAMP2 reverse, 5' –CCAGTTGCACCAGTCCTTGA-3'; mouse RAMP3 forward, 5'-ACCTGTCGGAGTTCATCG-3';

mouse RAMP3 reverse, 5'-ATCAGTGTGCTTGCTGCG-3'; mouse VEGF forward, 5'-CCCACGTCAGAGAGCAACATC-3'; mouse VEGF reverse, 5'-CTTTCTTTGGTCTGCATTCACATC-3'; mouse bFGF forward, 5'-AGCGGCTCTACTGCAAGAAC-3'; mouse bFGF reverse, 5'-GCCGTCCATCTTCCTTCATA-3'.

Statistical analysis

All values are expressed as means ± SD, unless stated otherwise. Group differences for hemodynamic, morphological, and general physiological measurements were analyzed for statistical significance by Student's t test or ANOVA. Statistical analysis for the 8-arm radial maze test was conducted using StatView (SAS Institute) and data were analyzed by two-way repeated measures ANOVA. Correlations between variables were analyzed with Pearson's coefficient. Differences with a probability value of $P<0.05$ were considered to be statistically significant.

Supporting information

High adrenomedullin level in the circulating blood in AM-Tg mice

The plasma concentrations of human total AM were 355.2±44.5 fmol/mL in AM-Tg mice but not detected in WT mice. The physiological concentration of mouse total AM reportedly ranges from 5 to 20 fmol/mL.[19, 20] Therefore, the transgenic mice were expected to overproduce AM at about 50 times the magnitude of endogenous AM. The systolic BP (mmHg) was 116.1±7.5 in WT mice (n=16), 105.6±6.5 in AM-Tg mice (n=16), and 102±3.9 in hydralazine-treated WT (H-WT) mice (n=8). **There were no apparent differences in overall appearance, behavior, growth, or fertility between wild-type and AM-Tg mice. The body weight (g) at 10–12 weeks old before the operation was 27.4±1.9 in WT mice (n=16), 26.5±1.4 in AM-Tg mice (n=16), and 27.1±1.7 in H-WT mice (n=8). There was no significant difference among the three groups.**

Supplemental References

1. Miyashita K, Itoh H, Arai H, Suganami T, Sawada N, Fukunaga Y, Sone M, Yamahara K, Yurugi-Kobayashi T, Park K, Oyamada N, Taura D, Tsujimoto H, Chao TH, Tamura N, Mukoyama M, Nakao K. The neuroprotective and vasculo-neuro-regenerative roles of adrenomedullin in ischemic brain and its therapeutic potential. *Endocrinology*. 2006;147:1642-1653

2. Shibata M, Ohtani R, Ihara M, Tomimoto H. White matter lesions and glial activation in a novel mouse model of chronic cerebral hypoperfusion. *Stroke*. 2004;35:2598-2603

3. Shibata M, Yamasaki N, Miyakawa T, Kalaria RN, Fujita Y, Ohtani R, Ihara M, Takahashi R, Tomimoto H. Selective impairment of working memory in a mouse model of chronic cerebral hypoperfusion. *Stroke*. 2007;38:2826-2832

4. Coltman R, Spain A, Tsenkina Y, Fowler JH, Smith J, Scullion G, Allerhand M, Scott F, Kalaria RN, Ihara M, Daumas S, Deary IJ, Wood E, McCulloch J, Horsburgh K. Selective white matter pathology induces a specific impairment in spatial working memory. *Neurobiol Aging*.

5. Iimuro S, Shindo T, Moriyama N, Amaki T, Niu P, Takeda N, Iwata H, Zhang Y, Ebihara A, Nagai R. Angiogenic effects of adrenomedullin in ischemia and tumor growth. *Circ Res*. 2004;95:415-423

6. Ayata C, Dunn AK, Gursoy OY, Huang Z, Boas DA, Moskowitz MA. Laser speckle flowmetry for the study of cerebrovascular physiology in normal and ischemic mouse cortex. *J Cereb Blood Flow Metab*. 2004;24:744-755

7. Shin HK, Jones PB, Garcia-Alloza M, Borrelli L, Greenberg SM, Bacskai BJ, Frosch MP, Hyman BT, Moskowitz MA, Ayata C. Age-dependent cerebrovascular dysfunction in a transgenic mouse model of cerebral amyloid angiopathy. *Brain*. 2007;130:2310-2319

8. Forrester KR, Stewart C, Tulip J, Leonard C, Bray RC. Comparison of laser speckle and laser

doppler perfusion imaging: Measurement in human skin and rabbit articular tissue. *Med Biol Eng Comput*. 2002;40:687-697

9. Maeda K, Hata R, Hossmann KA. Differences in the cerebrovascular anatomy of c57black/6 and sv129 mice. *Neuroreport*. 1998;9:1317-1319

10. Todo K, Kitagawa K, Sasaki T, Omura-Matsuoka E, Terasaki Y, Oyama N, Yagita Y, Hori M. Granulocyte-macrophage colony-stimulating factor enhances leptomeningeal collateral growth induced by common carotid artery occlusion. *Stroke*. 2008;39:1875-1882

11. Woitzik J, Hecht N, Schneider UC, Pena-Tapia PG, Vajkoczy P. Increased vessel diameter of leptomeningeal anastomoses after hypoxic preconditioning. *Brain Res*. 2006;1115:209-212

12. Schneider UC, Schilling L, Schroeck H, Nebe CT, Vajkoczy P, Woitzik J. Granulocyte-macrophage colony-stimulating factor-induced vessel growth restores cerebral blood supply after bilateral carotid artery occlusion. *Stroke*. 2007;38:1320-1328

13. Ergul A, Elgebaly MM, Middlemore ML, Li W, Elewa H, Switzer JA, Hall C, Kozak A, Fagan SC. Increased hemorrhagic transformation and altered infarct size and localization after experimental stroke in a rat model type 2 diabetes. *BMC Neurol*. 2007;7:33

14. Buschmann IR, Busch HJ, Mies G, Hossmann KA. Therapeutic induction of arteriogenesis in hypoperfused rat brain via granulocyte-macrophage colony-stimulating factor. *Circulation*. 2003;108:610-615

15. Palmer TD, Willhoite AR, Gage FH. Vascular niche for adult hippocampal neurogenesis. *J Comp Neurol*. 2000;425:479-494

16. Galvan V, Gorostiza OF, Banwait S, Ataie M, Logvinova AV, Sitaraman S, Carlson E, Sagi SA, Chevallier N, Jin K, Greenberg DA, Bredesen DE. Reversal of alzheimer's-like pathology and behavior in human app transgenic mice by mutation of asp664. *Proc Natl Acad Sci U S A*. 2006;103:7130-7135

17. Miyakawa T, Yamada M, Duttaroy A, Wess J. Hyperactivity and intact

hippocampus-dependent learning in mice lacking the m1 muscarinic acetylcholine receptor. *J Neurosci.* 2001;21:5239-5250

18. Hakuno D, Fukuda K, Makino S, Konishi F, Tomita Y, Manabe T, Suzuki Y, Umezawa A, Ogawa S. Bone marrow-derived regenerated cardiomyocytes (cmg cells) express functional adrenergic and muscarinic receptors. *Circulation.* 2002;105:380-386

19. Nambu T, Arai H, Komatsu Y, Yasoda A, Moriyama K, Kanamoto N, Itoh H, Nakao K. Expression of the adrenomedullin gene in adipose tissue. *Regul Pept.* 2005;132:17-22

20. Shindo T, Kurihara H, Maemura K, Kurihara Y, Kuwaki T, Izumida T, Minamino N, Ju KH, Morita H, Oh-hashi Y, Kumada M, Kangawa K, Nagai R, Yazaki Y. Hypotension and resistance to lipopolysaccharide-induced shock in transgenic mice overexpressing adrenomedullin in their vasculature. *Circulation.* 2000;101:2309-2316

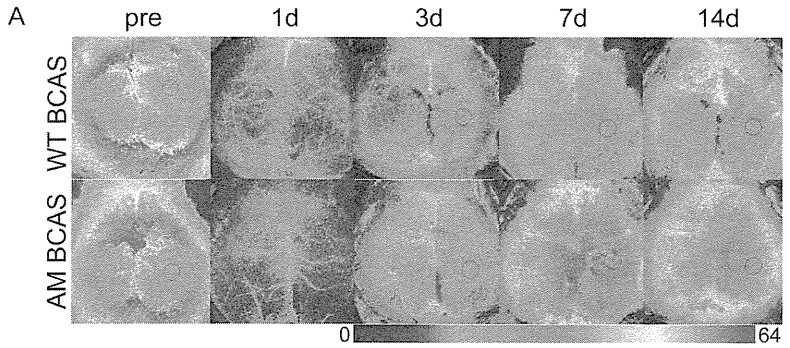

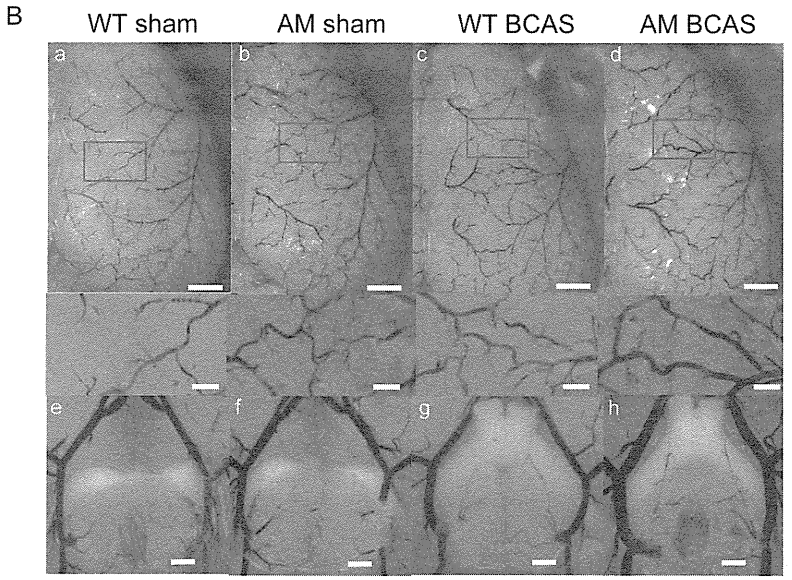

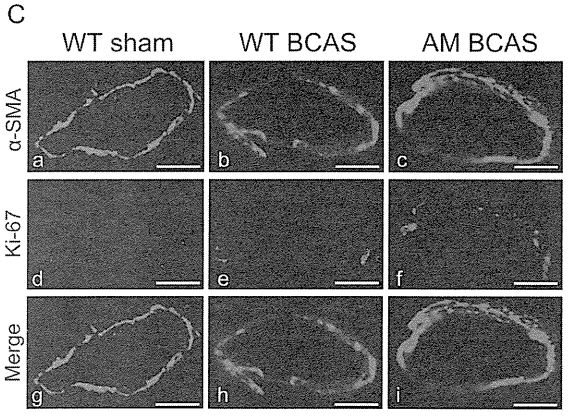

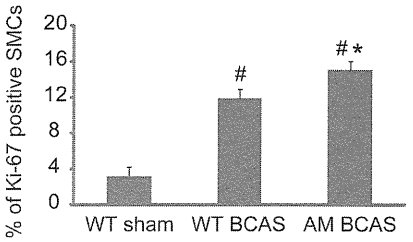

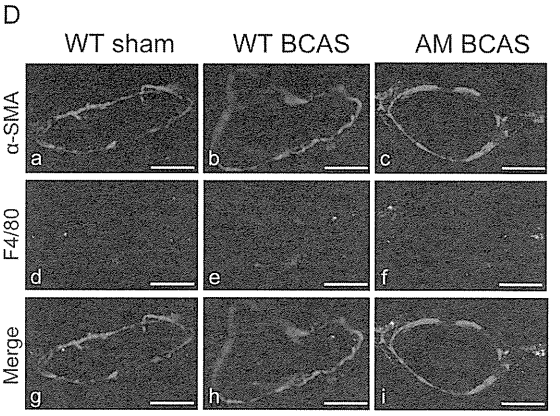

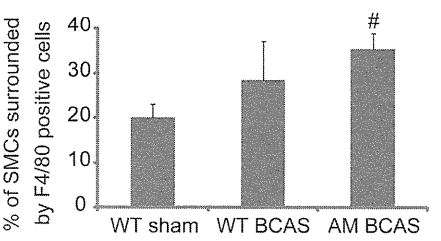

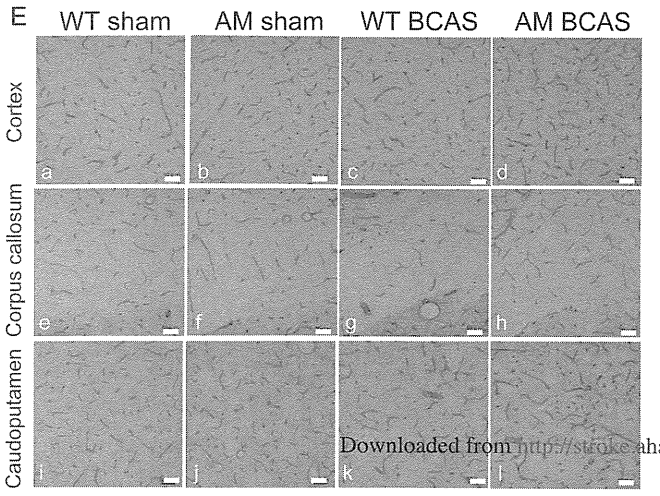

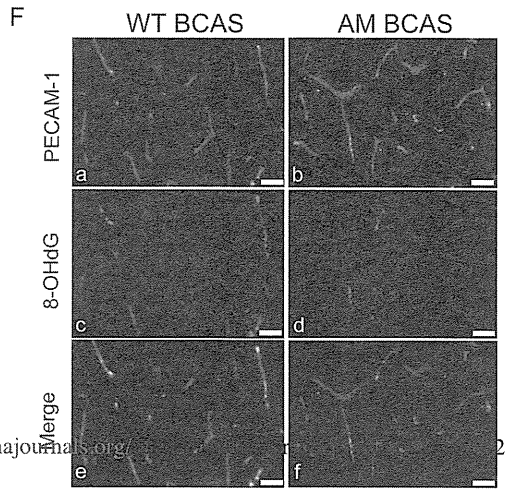

Supplemental Figure S1.

(A) Representative images showing temporal changes of CBF in wild-type (WT) and adrenomedullin (AM)-Tg mice after BCAS. (see Figure 1C for statistical analyses) (B) Representative images of the dorsal (a–d) and ventral (e–h) cerebral angioarchitecture by postmortem latex perfusion method of WT or AM-Tg mouse that is subjected to sham (WT sham or AM sham) or BCAS operation (WT BCAS or AM BCAS) on day 7. Scale bars, 1 mm (upper panels of a–d), 250 μm (lower panels of a–d), and 500 μm (e–h). (see Figure 2, C and D for statistical analyses) (C) Representative double immunofluorescence images for Ki-67 (green)/α-SMA (red) and their quantitative data of WT sham, WT BCAS, and AM BCAS on day 7. Scale bar, 10 μm (n=4 each). *P<0.05 in AM BCAS vs. WT BCAS; #P<0.05 vs. WT sham. (D) Representative double immunofluorescence images for F4/80 (green)/α-SMA (red) and their quantitative data of WT sham, WT BCAS, and AM BCAS on day 7. Scale bar, 10 μm (n=4 each). #P<0.05 vs. WT sham.

(E) Representative images of the PECAM-1-positive capillaries in sections from the cortex (a–d), the corpus callosum (e–h) and the caudoputamen (i–l) of WT sham, AM sham, WT BCAS, or AM BCAS on day 7. Scale bar, 50 μm. (see Figure 3C for statistical analyses) (F) Cerebral microvessels were stained for PECAM-1 and with 8-hydroxy-deoxyguanosine (8-OHdG). Representative images of sections from the corpus callosum of WT BCAS (a, c, e) or AM BCAS (b, d, f) on day 3. Scale bar, 50 μm. (see Figure 3D for statistical analyses)

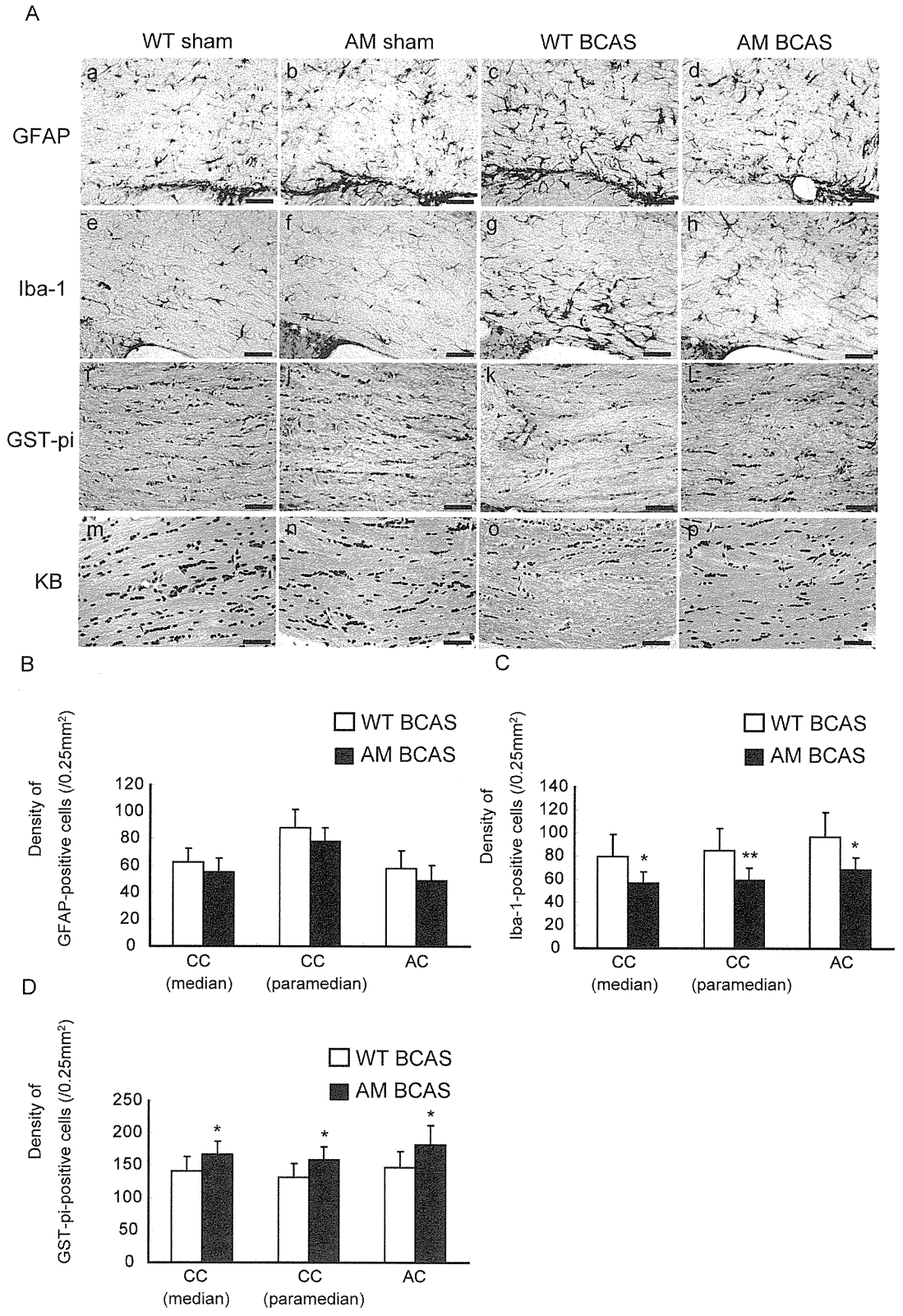

Supplemental Figure S2.

(A) Representative images of the corpus callosum of the immunohistochemical staining for GFAP (a–d), Iba-1 (e–h) and GST-pi (i–l) and the Klüver-Barrera (KB) staining (m–p) of wild-type or adrenomedullin (AM)-Tg mouse that is subjected to sham (WT sham or AM sham) or BCAS operation (WT BCAS or AM BCAS) on day 28. Scale bars, 50 μm. (see Figure 4 for statistical analyses) (B–D) Histograms showing the density of cells immunoreactive for GFAP (B), Iba-1 (C), or GST-pi (D) in the medial and paramedial portions of the corpus callosum (CC) and the anterior commissure (AC) of WT BCAS or AM BCAS on day 7 (n=7 each). Error bars indicate SD. *P<0.05, **P<0.01 in AM BCAS vs. WT BCAS.

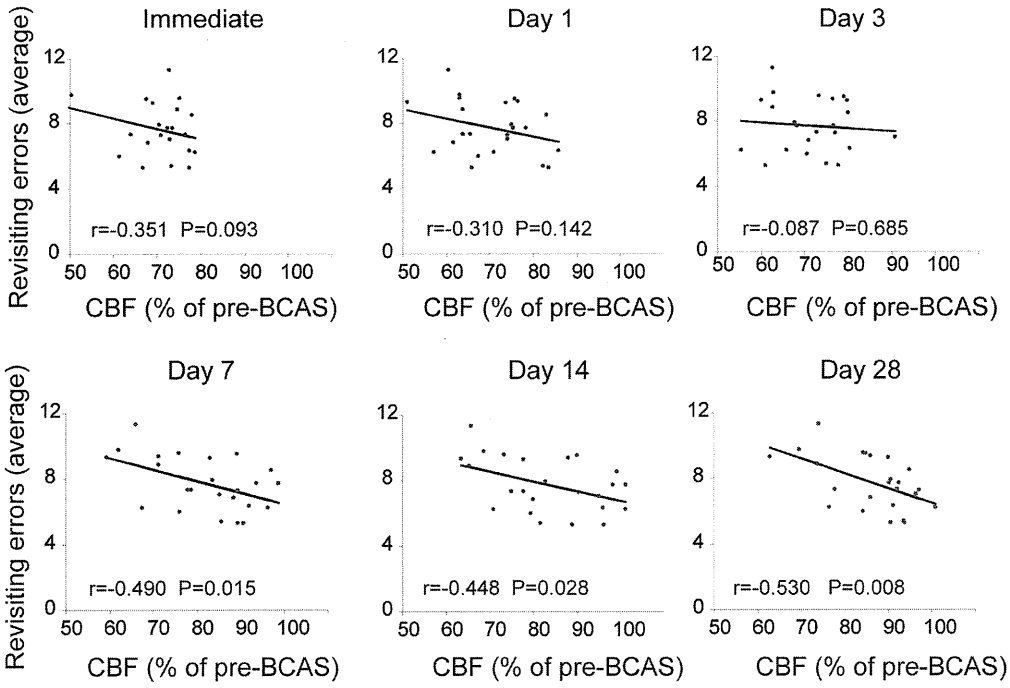

Supplemental Figure S3.

Correlation analysis between the cerebral blood flow (CBF) immediately after BCAS, as well as 1, 3, 7, 14, and 28 days after BCAS and the averaged number of revisiting errors (trial 1 to 26) at 1 month after BCAS (n=24).

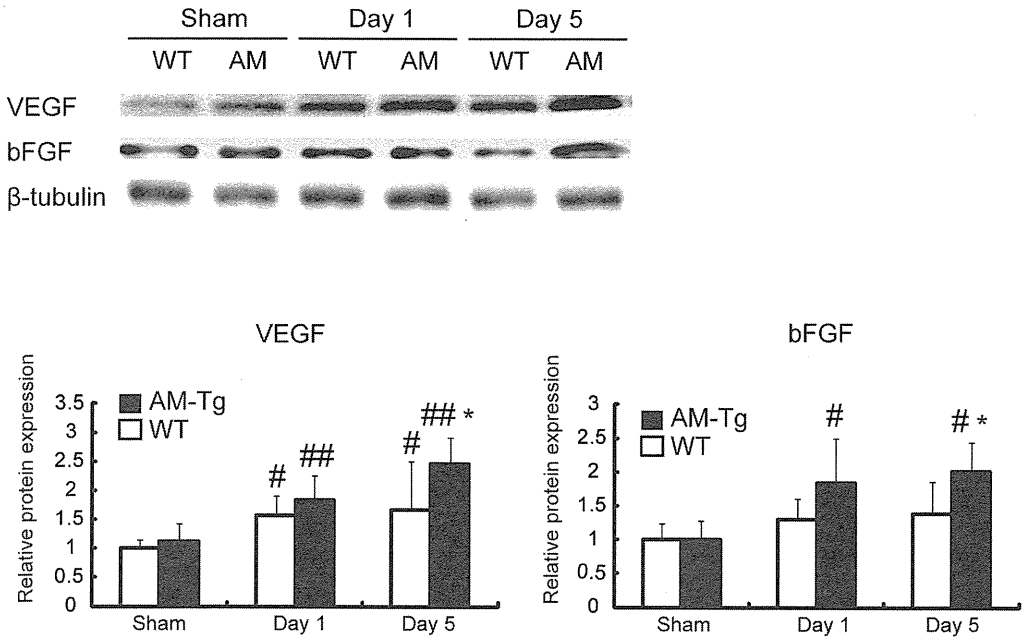

Supplemental Figure S4.

Western blotting of VEGF, bFGF, and β-tubulin (internal control) in extracts of the brain of wild-type or adrenomedullin (AM)-Tg mouse that is subjected to sham (WT sham or AM sham) or BCAS operation (WT BCAS or AM BCAS) on days 1 and 5 (n=6–8 each). Error bars indicate SD. *P<0.05 in AM BCAS vs. WT BCAS; #P<0.05 vs. WT sham.

Therapeutic Impact of Leptin on Diabetes, Diabetic Complications, and Longevity in Insulin-Deficient Diabetic Mice

Masaki Naito, Junji Fujikura, Ken Ebihara, Fumiko Miyanaga, Hideki Yokoi, Toru Kusakabe, Yuji Yamamoto, Cheol Son, Masashi Mukoyama, Kiminori Hosoda, and Kazuwa Nakao

OBJECTIVE—The aim of the current study was to evaluate the long-term effects of leptin on glucose metabolism, diabetes complications, and life span in an insulin-dependent diabetes model, the Akita mouse.

RESEARCH DESIGN AND METHODS—We cross-mated Akita mice with leptin-expressing transgenic (LepTg) mice to produce Akita mice with physiological hyperleptinemia (LepTg:Akita). Metabolic parameters were monitored for 10 months. Pair-fed studies and glucose and insulin tolerance tests were performed. The pancreata and kidneys were analyzed histologically. The plasma levels and pancreatic contents of insulin and glucagon, the plasma levels of lipids and a marker of oxidative stress, and urinary albumin excretion were measured. Survival rates were calculated.

RESULTS—Akita mice began to exhibit severe hyperglycemia and hyperphagia as early as weaning. LepTg:Akita mice exhibited normoglycemia after an extended fast even at 10 months of age. The 6-h fasting blood glucose levels in LepTg:Akita mice remained about half the level of Akita mice throughout the study. Food intake in LepTg:Akita mice was suppressed to a level comparable to that in WT mice, but pair feeding did not affect blood glucose levels in Akita mice. LepTg:Akita mice maintained insulin hypersensitivity and displayed better glucose tolerance than did Akita mice throughout the follow-up. LepTg:Akita mice had normal levels of plasma glucagon, a marker of oxidative stress, and urinary albumin excretion rates. All of the LepTg:Akita mice survived for >12 months, the median mortality time of Akita mice.

CONCLUSIONS—These results indicate that leptin is therapeutically useful in the long-term treatment of insulin-deficient diabetes. ***Diabetes*** **60:2265–2273, 2011**

Leptin is an adipocyte-derived hormone that is involved in the regulation of food intake and energy expenditure (1). We previously created transgenic mice that overexpress leptin under the control of the liver-specific promoter (LepTg) (2). The plasma leptin level is stable in LepTg mice and similar to that in obese rodents and humans, suggesting that the phenotypic changes found in these animals are physiologically relevant (3,4). LepTg mice provide a unique experimental system to investigate the chronic in vivo effects of leptin. LepTg mice exhibit increased glucose metabolism, which is accompanied by the activation of insulin signaling in skeletal muscle and the liver (2). These findings indicate that leptin acts as an antidiabetic hormone. We have demonstrated the efficacy of leptin in various mouse models of diabetes (5–8).

Akita mice are an animal model of diabetes caused by pancreatic β-cell failure. Endoplasmic reticulum stress induced by misfolded proinsulin is responsible for the β-cell dysfunction and destruction in Akita mice. Male Akita mice start to develop hyperglycemia as early as weaning, when 71% decrease of β-cell mass is present. Plasma insulin levels in the mice are reduced to 41% of the control mice at 7 weeks of age. The blood glucose levels in male Akita mice increase irreversibly up to 700 mg/dL at 10 weeks of age, and about half the male Akita mice die of extreme hyperglycemia within the 1st year of life (9). Thus, the Akita mouse is a suitable model for evaluating the therapeutic impact of interventions on the onset, progression, and prognosis of diabetes.

In the current study, to clarify how and to what extent chronic leptin therapy affects the long-term course of diabetes, we genetically crossed LepTg and Akita mice to create a unique mouse model of nonobese diabetes with elevated plasma leptin level. Using this mouse diabetes model, we investigated the chronic lifelong effects of leptin on diabetes, diabetic nephropathy, and longevity in Akita mice.

RESEARCH DESIGN AND METHODS

Animals. Generation of LepTg mice was reported previously (2). Briefly, a fusion gene comprising the human serum amyloid P component promoter upstream of the mouse leptin cDNA coding sequences was designed to target hormone expression to the liver (2,8). The highest expressing transgenic line was used in this study (2). The genotype for LepTg mice was determined by PCR (5′-GCTGGTTGTTGTGCTGTCTC-3′; 5′-CAGGCTGGTGAGGACCTGTT-3′). B6-Ins2Akita (*Ins2*$^{WT/C96Y}$; referred to hereafter as Akita) mice were purchased from Japan SLC (Shizuoka, Japan). Presence of the Akita mutation was verified by absence of an Fnu4HI restriction site in the PCR product of the *Ins2* gene (5′-TGCTGATGCCCTGGCCTGCT-3′; 5′-TGGTCCCACATATGCACATG-3′). Both LepTg and Akita mice were on the same C57BL/6 J background. Hemizygous male LepTg mice were cross-mated with female heterozygous Akita mice. Male F1 mice were used in this study. Mice were maintained in a temperature-, humidity-, and light-controlled room and allowed free access to standard diet (F-2 diet; Oriental BioService, Kyoto, Japan).

The care of the animals and all experimental procedures were conducted in accordance with the guidelines for animal experiments of Kyoto University and were approved by the Animal Research Committee of Kyoto University.

Metabolic parameters measurements. Levels of leptin (Mouse Leptin ELISA, Millipore, St. Charles, MO), glucose (Glutest Neo Super, Sanwa, Nagoya, Japan, or Glucose C2-test, Wako, Osaka, Japan), HbA_{1c} (DCA2000 analyzer, Bayel-Sankyo, Tokyo, Japan), insulin (Ultra-Sensitive PLUS Mouse Insulin Kit, Morinaga, Yokohama, Japan), glucagon (Glucagon EIA Kit, Yanaihara, Shizuoka, Japan), triglyceride (TG; Triglyceride E-test, Wako), nonesterified fatty acid (NEFA; NEFA C-test, Wako), β-hydroxybutyrate (Precision Xtra, Abbott, Bedford, MA), and thiobarbituric acid reactive substances (TBARS; TBARS

From the Department of Medicine and Clinical Science, Kyoto University Graduate School of Medicine, Kyoto, Japan.
Corresponding author: Junji Fujikura, j-fuji@sannet.ne.jp.
Received 30 December 2010 and accepted 24 June 2011.
DOI: 10.2337/db10-1795

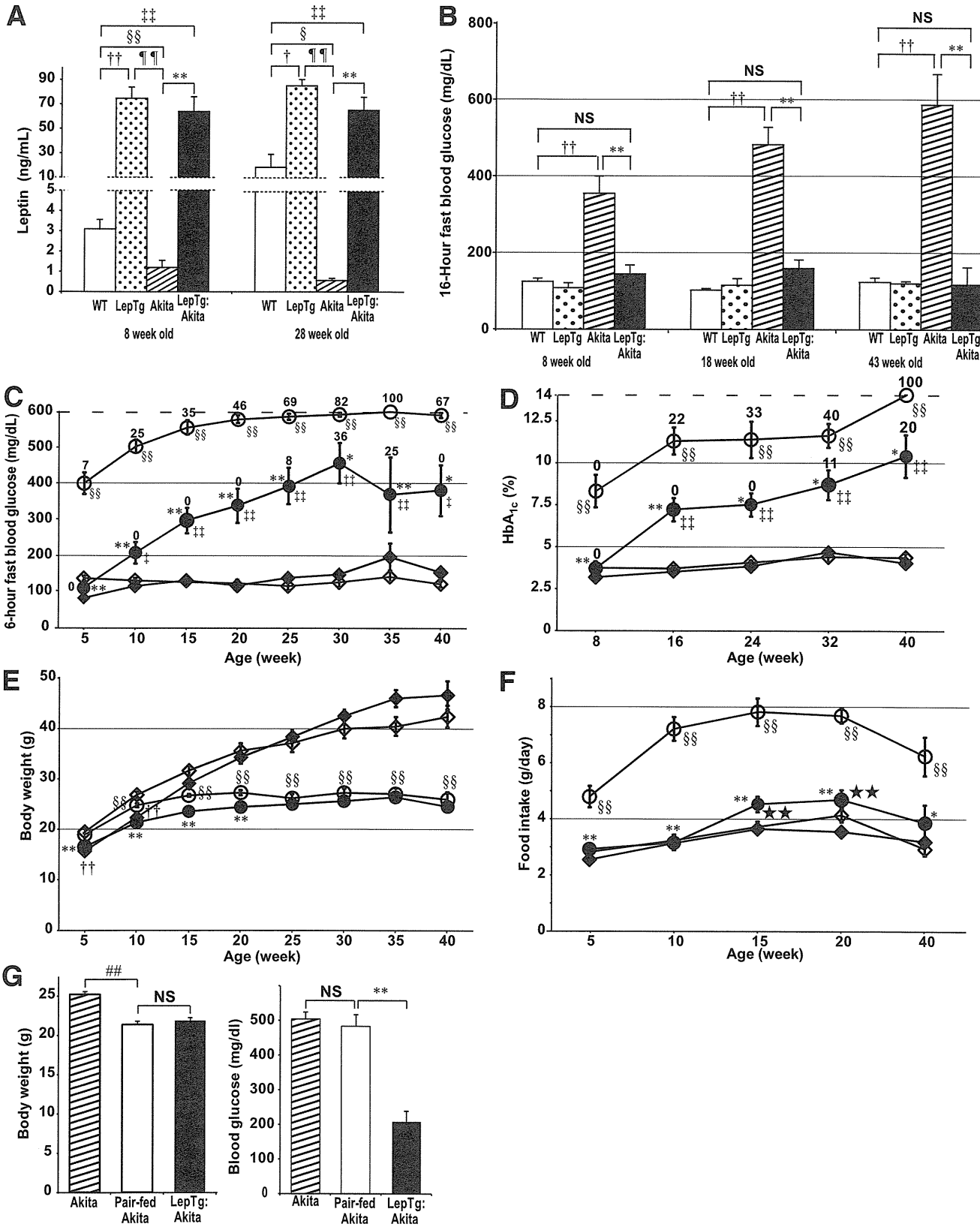

FIG. 1. Time course of changes in plasma leptin, blood glucose, HbA_{1c}, body weight, and food intake. *A*: Plasma leptin levels of WT, LepTg, Akita, and LepTg:Akita mice at 8 and 28 weeks of age ($n \geq 4$ in each group). *B*: Sixteen-hour fasting blood glucose levels of WT, LepTg, Akita, and LepTg: Akita mice at 8, 18, and 43 weeks of age ($n \geq 4$ in each group). *C*: Time course of 6-h fasting blood glucose concentrations of WT (◇), LepTg (◆), Akita (○), and LepTg:Akita (●) mice ($n \geq 11$ in each group, except $n = 5$ for data of 40 weeks of age). Since the glucometer has a detection limit up to 600 mg/dL, values above the detection limit were treated as 601 mg/dL. Dashed line indicates detection limit of 600 mg/dL. The numbers along the curves indicate the percent of samples above detection limit. *D*: Time course of glycated hemoglobin (HbA_{1c}) levels of WT (◇), LepTg (◆), Akita (○), and LepTg:Akita (●) mice ($n \geq 4$ in each group). Since the analyzer has a detection limit up to 14%, values above the detection limit were treated as 14.1%. Dashed line indicates detection limit of 14%. The numbers along the curves indicate the percent of samples above detection limit.

Assay Kit, Cayman, Ann Arbor, MI) were measured. Percent body fat was measured by Latheta LTC-100 (ALOKA, Tokyo, Japan). For glucose tolerance tests (GTTs), after 12-h fast, the mice were injected with 1.0 g/kg i.p. glucose. For insulin tolerance tests (ITTs), after a 6-hour fast, the mice were injected with 0.5 units/kg i.p. human insulin (Novo Nordisk, Bagsvaerd, Denmark).

Pair-feeding experiment. Akita mice were given the amount of food consumed by ad libitum–fed LepTg:Akita mice on the previous day. A pair-feeding study was conducted from 8 through 11 weeks of age. Body weights and blood glucose concentrations were measured at the end of the period.

Pancreatic hormone secretion and content. After 12-h fast, the mice were injected with 3.0 g/kg i.p. glucose. Blood samples were obtained from the retro-orbital venous sinus using heparin-coated glass capillaries. For hormone content, pancreata were homogenized in acid ethanol.

Histology. Pancreata were fixed in 4% paraformaldehyde and embedded in paraffin. Sections were immunostained with the following antibodies: guinea pig anti-insulin antibody (Dako, Glostrup, Denmark), rabbit antiglucagon antibody (Dako), and Alexa488 anti–guinea pig antibody and Alexa546 anti-rabbit antibody (both from Molecular Probes, Eugene, OR). Kidney tissues were fixed in 4% paraformaldehyde and embedded in paraffin. Periodic acid Schiff (PAS) was used to stain 1-μm sections. Mesangial area was determined by the presence of PAS-positive and nuclei-free area in the mesangium. Measurement of the mesangial area of more than 22 glomeruli randomly selected in each mouse was performed with a computer-assisted microscopy (Keyence, Osaka, Japan).

Albumin in urine. A metabolic cage was used to collect 24-h urine. Urinary albumin concentration was measured using Albuwell M (Exocell, Philadelphia, PA). Blood pressure was measured by the indirect tail-cuff method.

Survival rates. Survival data were analyzed by Kaplan-Meier analysis, and comparisons between genotypes were done by the log-rank test.

Statistical analyses. Data are expressed as means ± SE. Comparison between or among groups was by Student *t* test, Mann-Whitney *U* test, or ANOVA with Scheffé *F* test. $P < 0.05$ was considered statistically significant.

RESULTS

Generation of LepTg:Akita mice. Plasma leptin levels were measured periodically (Fig. 1*A*). At 8 weeks of age, the plasma leptin levels in Akita mice declined to 39% of the levels in WT mice (3.1 ng/mL for WT vs. 1.2 ng/mL for Akita; $P < 0.01$). Five months later, at 28 weeks of age, an age-dependent increase in plasma leptin levels in WT mice and decrease in Akita mice were observed (18.8 ng/mL for WT vs. 0.58 ng/mL for Akita; $P < 0.05$). The transgenic expression of leptin was associated with markedly and stably increased plasma leptin levels in both LepTg and LepTg:Akita mice (74.8 ng/mL for LepTg and 64.2 ng/mL for LepTg:Akita at 8 weeks of age and 85.1 ng/mL for LepTg and 65.3 ng/mL for LepTg:Akita at 28 weeks of age).

Time course of changes in blood glucose and HbA_{1c} levels. Blood glucose levels were measured after a 16-h fast at 8, 18, and 43 weeks of age (Fig. 1*B*). Akita mice showed hyperglycemia with blood glucose levels >300 mg/dL even after the 16-h fast at 8 weeks of age, and this hyperglycemia worsened progressively with time. By contrast, the glucose levels remained <160 mg/dL and were indistinguishable between LepTg:Akita and WT mice at all times studied.

Six-hour fasting blood glucose levels, which correlate closely with the daily averaged blood glucose level, and HbA_{1c} levels were followed for ~10 months (Fig. 1*C* and *D*) (10). In Akita mice, 6-h fasting blood glucose levels were >500 mg/dL after 10 weeks of age, and more than half of the mice had blood glucose levels >600 mg/dL after 15 weeks of age (Fig. 1*C*). The blood glucose levels were lower in LepTg:Akita mice than in WT mice at 5 weeks of age and increased gradually after 10 weeks of age but remained <400 mg/dL at 40 weeks of age (Fig. 1*C*). Average 6-h fasting blood glucose levels were 552.4 ± 24.1 mg/dL in Akita, 321.0 ± 39.6 mg/dL in LepTg:Akita, 136.3 ± 11.8 mg/dL in LepTg, and 128.7 ± 3.0 mg/dL in WT mice from 5 to 40 weeks of age. Thus, the average blood glucose level in LepTg:Akita mice was ~58.1% of that in Akita mice.

HbA_{1c} levels changed in a similar pattern to the 6-h fasting blood glucose levels (Fig. 1*D*). By 8 weeks of age, Akita mice had markedly elevated HbA_{1c} levels (8.4 ± 1.0%), whereas HbA_{1c} levels were the same in LepTg:Akita mice (3.7 ± 0.1%) as in WT mice (3.8 ± 0.4%) at that age. Of Akita mice >16 weeks of age, >22% had HbA_{1c} levels above the detection limit (14%). The HbA_{1c} levels of LepTg:

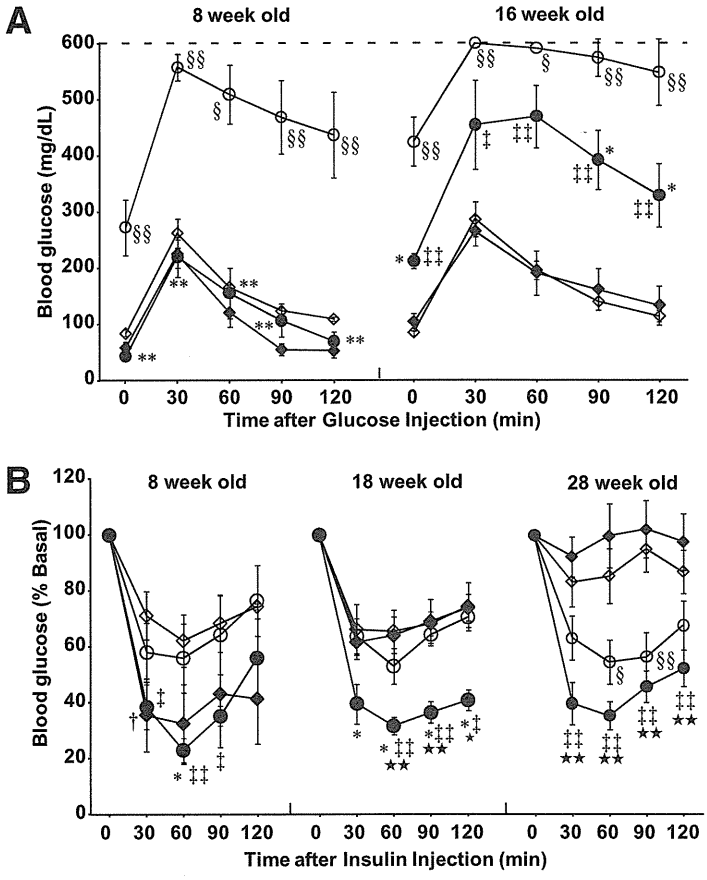

FIG. 2. GTTs and ITTs. *A*: GTTs of WT (◇), LepTg (◆), Akita (open circles), and LepTg:Akita (closed circles) mice at 8 and 16 weeks of age. Blood glucose levels are shown at indicated times after glucose injections (1 g/kg body wt i.p.; $n \geq 4$ in each group). *B*: ITTs of WT (◇), LepTg (◆), Akita (○), and LepTg:Akita (●) mice at 8, 18, and 28 weeks of age. Percent changes in blood glucose levels are shown at indicated times after injection of insulin (0.5 units/kg body wt i.p.; $n \geq 4$ in each group). Dashed line indicates detection limit of 600 mg/dL. Data are expressed as means ± SE. §$P < 0.05$, §§$P < 0.01$ for WT vs. Akita, ‡$P < 0.05$, ‡‡$P < 0.01$ for WT vs. LepTg:Akita, ★$P < 0.05$, ★★$P < 0.01$ for LepTg vs. LepTg:Akita, *$P < 0.05$, and **$P < 0.01$ for Akita vs. LepTg:Akita.

***E*: Time course of body weight changes of WT (◇), LepTg (◆), Akita (○), and LepTg:Akita (●) mice ($n \geq 11$ in each group, except $n = 5$ for data of 40 weeks of age). *F*: Time course of 24-h food intake of WT (◇), LepTg (◆), Akita (○), and LepTg:Akita (●) mice ($n \geq 11$ in each group, except $n = 4$ for data of 40 weeks of age). *G*: Body weight of Akita, pair-fed Akita, and LepTg:Akita mice at the end of 3 weeks of pair feeding ($n = 4$ in each group). *H*: Six-hour fasting blood glucose concentrations of Akita, pair-fed Akita, and LepTg:Akita mice at the end of 3 weeks of pair feeding ($n = 4$ in each group). Data are expressed as means ± SE. In *A–F*, †$P < 0.05$, ††$P < 0.01$ for WT vs. LepTg, §$P < 0.05$, §§$P < 0.01$ for WT vs. Akita, ‡$P < 0.05$, ‡‡$P < 0.01$ for WT vs. LepTg:Akita, ¶¶$P < 0.01$ for LepTg vs. Akita, ★★$P < 0.01$ for LepTg vs. LepTg:Akita, *$P < 0.05$, and **$P < 0.01$ for Akita vs. LepTg:Akita. In *G* and *H*, ##$P < 0.01$ for Akita vs. pair-fed Akita and **$P < 0.01$ for LepTg:Akita vs. pair-fed Akita.**

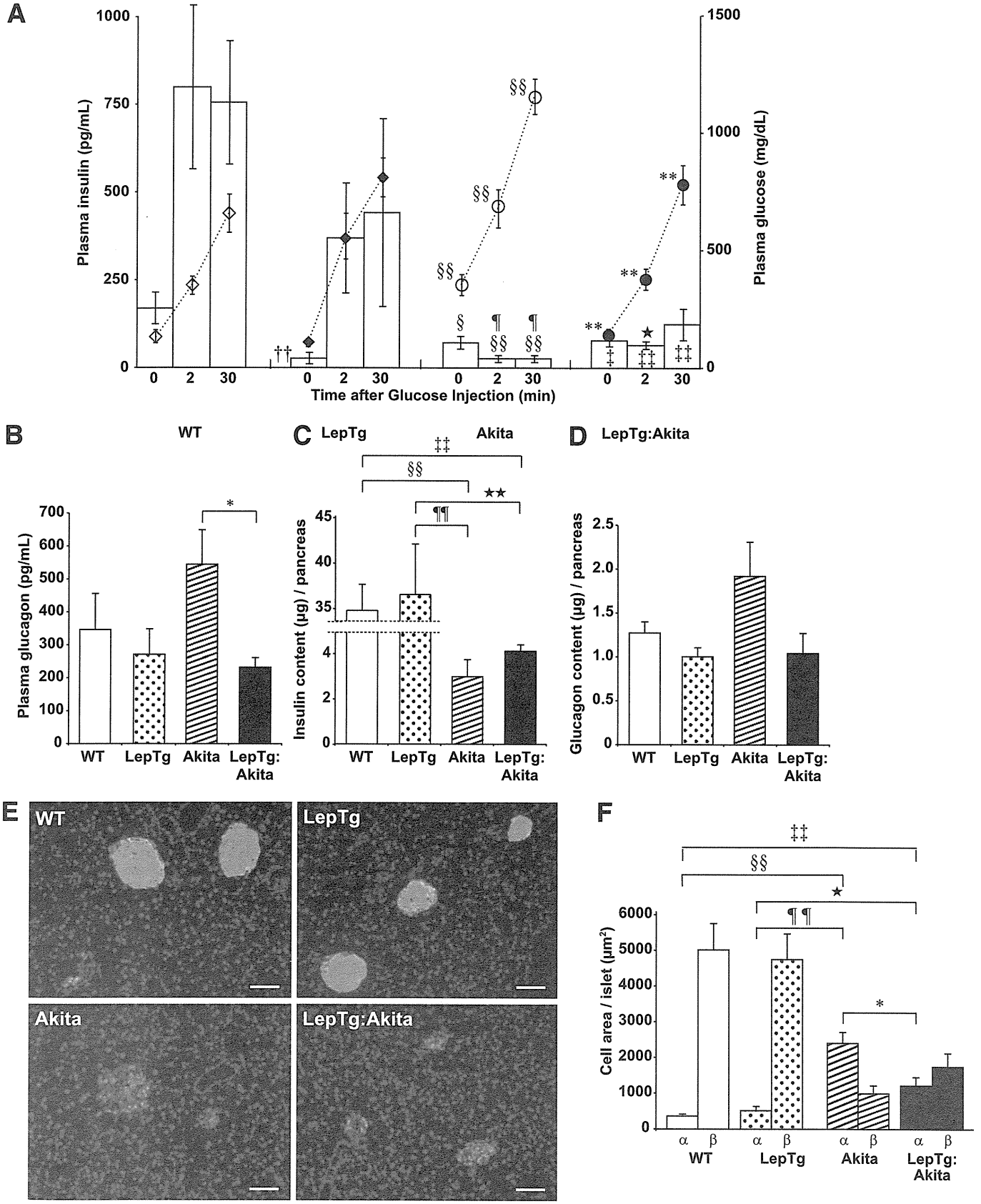

FIG. 3. Glucose-stimulated insulin secretion, plasma glucagon levels, and pancreatic hormone contents. *A*: Plasma insulin (open bars) and glucose (black lines) concentrations after glucose (3 g/kg i.p.) injection in WT, LepTg, Akita, and LepTg:Akita mice at 8 weeks of age ($n \geq 4$ in each group). *B*: Plasma glucagon concentration in ad libitum–fed WT, LepTg, Akita, and LepTg:Akita mice at 22 weeks of age ($n \geq 4$ in each group). *C* and *D*: Pancreatic insulin (*C*) and glucagon (*D*) content measured in acid-ethanol extracts of homogenized pancreas from WT, LepTg, Akita, and LepTg:Akita mice at 18 weeks of age ($n \geq 5$ in each group). *E*: Double immunofluorescent stainings against insulin (green) and glucagon (red) in pancreatic sections from WT, LepTg, Akita, and LepTg:Akita mice at the age of 18 weeks. Scale bar indicates 50 μm. *F*: α-Cell and β-cell areas per islet